

# Signal Design and Convolutional Coding for Noncoherent Space–Time Communication on the Block-Rayleigh-Fading Channel

Michael L. McCloud, *Member, IEEE*, Matthias Brehler, *Student Member, IEEE*, and Mahesh K. Varanasi, *Senior Member, IEEE*

**Abstract**—We consider the problem of designing signal constellations for the multiple transmit–multiple receive antenna Rayleigh-fading communication channel, when neither the transmitter nor the receiver know the fading. In particular, by employing the asymptotic union bound (AUB) on the probability of error, we give a new formulation of the problem of signal design for the noncoherent fading channel. Since unitary signals are optimal for this channel (in the limit of large signal-to-noise ratios SNRs), the problem can be posed in terms of packings on the Grassmannian manifold. A key difference in our approach from that of other authors is that we use a notion of distance on this manifold that is suggested by the union bound. As a consequence of our use of this distance measure, we obtain signal designs that are guaranteed to achieve the full diversity order of the channel, a result that does not hold when the chordal distance is used. We introduce a new method of recursively designing signals, termed successive updates, to approximately optimize this performance measure. We then examine the use of our signals with several convolutional codes over the fading channel. An upper bound on the bit error probability of the maximum-likelihood decoder is presented together with an asymptotic analysis of that bound.

**Index Terms**—Convolutional coding, fading channels, noncoherent communication, signal design, space–time modulation.

## I. INTRODUCTION

**I**N this paper, we consider the problem of designing signal waveforms for use with multiple transmit and receive antennas over the wireless block-fading channel, also known as space–time communication. This problem has received considerable attention, due in large part to the information-theoretical work of Telatar, Foschini, and Gans [1], [2], who showed that the use of transmit *and* receive antenna diversity could achieve considerable gains on the Rayleigh-fading channel when the receiver has perfect side information about the channel state. This work was later extended to the noncoherent channel where the receiver is not allowed this side information in [3]. In that paper, the capacity-achieving signals are shown to be the product of

an isotropically distributed unitary matrix with an independent real, nonnegative diagonal energy matrix (when the fading coefficients, associated with each transmit/receive antenna pair are independent and identically distributed (i.i.d.)). For high signal-to-noise ratio (SNR), Zheng and Tse [4] show that the capacity-maximizing signals are of equal energy and relate the problem to sphere packing on the Grassmann manifold. The common theme in these papers is that diversity communications can yield significant improvements over single-antenna communications, when designed intelligently.

In this and the previously mentioned papers, the channel is assumed to be fixed for  $D$  time slots<sup>1</sup> and then changes independently to another realization in the next  $D$  time slots, and so on. Physically, such a situation may arise for example in frequency-hopped systems. On the other hand, when the channel is assumed to be (essentially) constant for any two consecutive (block-) channel uses, noncoherent reception in multiantenna channels can also be achieved with differential encoding and detection and various signal designs have been suggested to this end [6]–[10]. We do not consider such slowly changing channels, but focus on signal designs for the block-fading channel with independent channel realizations for each block.

As a signal design criterion we choose to minimize the *asymptotic union bound* (AUB) on the symbol error rate (SER), derived for the single-antenna channel in [11] and for the general space–time channel in [5]. This criterion depends on all of the pairwise error probabilities, which in turn admit asymptotically tight expressions for channel models in which even correlated fading (across antennas) may be present. Previously, a Chernoff bound was used to upper-bound the pairwise error probability [12]. Based on the worst case distance between any two signals (as calculated through the Chernoff upper bound), a simple design algorithm is developed in [12] that is suitable for small cardinality constellations. Note that while the worst case exact pairwise error probability may be a reasonable (i.e., not too loose) lower bound on the SER of the signal set,<sup>2</sup> by upper-bounding it with a Chernoff bound, no statement

Manuscript received November 15, 2000; revised September 14, 2001. This work was supported in part by ARO under Grant DAAD19-99-1-0291 and by NSF under Grants ANI-9725778 and ECS-9979400.

M. L. McCloud was with the Department of Electrical and Computer Engineering, University of Colorado, Boulder, CO 80309-0425 USA. He is now with Magis Networks Inc., San Diego, CA 92130 USA (e-mail: mccloud@ieee.org).

M. Brehler and M. K. Varanasi are with the Department of Electrical and Computer Engineering, University of Colorado at Boulder, Boulder, CO 80309-0425 USA (e-mail: brehler@dsp.colorado.edu; varanasi@colorado.edu).

Communicated by G. Caire, Associate Editor for Communications.

Publisher Item Identifier S 0018-9448(02)03096-1.

<sup>1</sup>This terminology implies a basis of time translates of a single waveform (so that  $D$  corresponds to the length of the coherence interval in symbol durations), which, while commonly used, is restrictive [5].

<sup>2</sup>The reliance on the worst case error event appears to be based on insight from the additive white Gaussian noise channel, where the exponential nature of the pairwise error probabilities leads to this measure as it provides an asymptotically tight lower bound. This is not the case on the Rayleigh-fading channel, however, because the pairwise error probabilities are *polynomial* in the reciprocal of the SNR.

can be made as to whether or not this is a lower or an upper bound. Luckily, however, for high SNRs, the Chernoff bound displays the same dependence on the two signals as the asymptotically tight expressions found in [5], [11], so that at least asymptotically, signals are designed by minimizing a lower bound on the SER. However, in [13] and [14] the Chernoff bound on the pairwise error probability is further loosened by upper-bounding it [13, eq. (10)] to finally arrive at the minimum chordal distance (the precise definition of which is found in Section IV) between any two signals as the design criterion to be optimized [14] ([13] uses a different but equivalent design criterion). How this upper bound on the Chernoff bound used in a lower bound on SER (worst pairwise error probability) relates to the true SER (minimization of which should be the ultimate goal of signal design) is not discussed in those references. We provide an example in Section VI-A in this paper that shows that signal sets designed according to the maximization of the minimum chordal distance do not guarantee full transmit diversity, indicating its limited validity. On the other hand, the minimization of a strict asymptotic upper bound on SER, the AUB, may be more conservative but offers a solid relation to the true SER and assures full transmit diversity.

All signal designs for the noncoherent space–time channel constrain the signals to be “unitary” (the signals transmitted across the  $M$  transmit antennas are orthonormal in time) and so do we. The use of unitary signals is justified from information-theoretic arguments in [3], [4] and from error probability arguments in [5], at least for large values of the SNR. Interestingly, in [5] it is shown that the AUB is always minimized by unitary signals (under the assumption of equal-energy signals), whether the fading is correlated (across antennas) or, as is usually assumed, independent and identically distributed. The restriction to unitary signals enables a description of the signal set using a parameterization of the Grassmann manifold,  $G(M, D)$  (the space of all  $M$ -dimensional subspaces of the  $D$ -dimensional complex space  $\mathbb{C}^D$ ), first used and suggested in [14].

In [13], the unitary structure of the signals is exploited by starting with the first signal and systematically rotating it. Alternatively, the same signal constellations can also be generated by mapping a linear block code over the ring of integers into complex signal matrices. Either way, the signals are systematically generated. The design algorithm, however, randomly searches over the generating matrices of the block code, evaluating the minimum chordal distance for each code and picking the one which maximizes this measure.

In [14], the problem of noncoherent space–time signal design is formulated as a sphere-packing problem over the Grassmann manifold. By using chordal distance as the design criterion, the authors of that paper are able to extend results from the coherent version of this problem, developed in [15], to the space–time context. They subsequently profit from some of the existing packings and optimization “machinery” for the Grassmann manifold  $G(M, D)$  with chordal distance. Nevertheless, the maximization of the  $l_\infty$  objective (minimum chordal distance) considered there is numerically difficult and the objective does not guarantee full transmit diversity, a potential shortcoming it shares with [13].

In contrast, the AUB provides a smooth objective function that guarantees full transmit diversity. In Section IV, we pose the signal design problem in terms of a parameterization of the Grassmann manifold. The joint optimization of the signals becomes numerically intractable for higher spectral efficiencies and diversity orders. For this reason, we introduce a new technique, called successive updates, which exploits the structure of the AUB to obtain a fast, recursive, suboptimal solution technique. Several examples are presented that demonstrate the utility of this new technique. There are two key differences between our approach and that of [13] and [14]. The first one is that we use a distance measure on  $G(M, D)$  which is determined by a product of functions of the principal angles between subspaces rather than the sum of these terms (the chordal distance between subspaces). This guarantees full diversity order on the space–time channel and is the quantity suggested by both the AUB *and* the Chernoff bound on the pairwise error probabilities at large SNRs. The second difference is that we use an average error criterion, rather than a measure that is inspired by the worst case pairwise error probability.

In addition to the new design method, we explore the use of convolutional codes in conjunction with our designs in Section VII. We examine rate- $1/Q$  convolutional codes presented for use with orthogonal signals in [16]. Numerical results indicate that by allowing correlation among the continuous-time encoding waveforms (namely, the space–time signals), we can improve the spectral efficiency of the system at a fixed error rate with small losses in energy efficiency.

## II. THE RAYLEIGH-FADING CHANNEL

We adopt the usual block-fading channel model for space–time communications in  $D$  dimensions with  $M$  transmit and  $N$  receive antennas, wherein the discrete time received signal at the  $n$ th antenna is of the form

$$\mathbf{y}_n = \sqrt{\bar{\gamma}} \mathbf{S}_i \mathbf{h}_n + \mathbf{n}_n. \quad (1)$$

Here  $\mathbf{S}_i \in \mathbb{C}^{D \times M}$  is the  $i$ th signal from a set of cardinality  $S$ ,  $\mathbf{h}_n \in \mathbb{C}^{M \times 1}$  is the vector of fading coefficients from each transmit antenna to sensor  $n$ , and  $\mathbf{n}_n$  is additive noise.

Stacking the  $D$  observations per receiver antenna yields the  $DN$  sufficient statistics

$$\mathbf{y} = [\mathbf{y}_1^\top, \dots, \mathbf{y}_N^\top]^\top = \sqrt{\bar{\gamma}} \mathbf{S}_i \mathbf{h} + \mathbf{n} \quad (2)$$

where  $\mathbf{S}_i = \mathbf{I}_N \otimes \mathbf{S}_i$  ( $\otimes$  is the Kronecker product [17] and  $\mathbf{I}_N$  is the  $N \times N$  identity matrix),  $\mathbf{h} = [\mathbf{h}_1^\top, \dots, \mathbf{h}_N^\top]^\top$ , and  $\mathbf{n} = [\mathbf{n}_1^\top, \dots, \mathbf{n}_N^\top]^\top$ . We assume that the additive noise is spatially white, but the fading need not be, i.e.,  $\boldsymbol{\Sigma} = E[\mathbf{h}\mathbf{h}^*]$  need not be diagonal (the superscript  $*$  denotes the complex conjugate transpose operation). In this model, we normalize the noise so that  $E[\mathbf{n}\mathbf{n}^*] = \mathbf{I}$ , the signals so that  $\text{tr}\{\mathbf{S}_i^* \mathbf{S}_i\} = M$ , and the fading process so that  $E[\mathbf{h}_n^* \mathbf{h}_n] = 1$  (for i.i.d. fading this amounts to  $M\boldsymbol{\Sigma} = \mathbf{I}$ ). We further assume that “unitary” signals are used so that  $\mathbf{S}_i^* \mathbf{S}_i = \mathbf{I}$ . Consequently, the scalar  $\bar{\gamma} = \frac{E_s}{N_0}$  denotes the average signal-to-noise ratio (SNR) at each receiver, independent of the number of transmit antennas  $M$ .

Conditioned on the transmission of signal  $\mathcal{S}_i$ , and denoting the determinant of a matrix  $\mathbf{X}$  as  $|\mathbf{X}|$ , the measurement has likelihood function

$$f_i(\mathbf{y}) = \frac{\exp\left\{-\mathbf{y}^* (\mathbf{I}_{DN} + \bar{\gamma} \mathcal{S}_i \Sigma \mathcal{S}_i^*)^{-1} \mathbf{y}\right\}}{\pi^{ND} |\mathbf{I}_{DN} + \bar{\gamma} \mathcal{S}_i \Sigma \mathcal{S}_i^*|}. \quad (3)$$

The optimal detection strategy is the maximum likelihood rule<sup>3</sup>

$$\begin{aligned} \phi^{ML}: \hat{i} &= \arg \max_i f_i(\mathbf{y}) \\ &= \arg \max_i \mathbf{y}^* \mathcal{S}_i \left(\mathbf{I}_{DN} + \bar{\gamma}^{-1} \Sigma^{-1}\right)^{-1} \mathcal{S}_i^* \mathbf{y} \end{aligned} \quad (4)$$

where we have applied a matrix inversion identity [17] to the quadratic form in the likelihood function.

### III. PERFORMANCE OF THE MAXIMUM LIKELIHOOD DETECTOR

To evaluate the probability of error for the maximum-likelihood test of (4) we employ a union upper bound on the probability of error

$$P \leq \frac{1}{S} \sum_{i=1}^S \sum_{\substack{k=1 \\ i \neq k}}^S P_{i,k} \quad (5)$$

where  $P$  is the probability of a symbol error and  $P_{i,k}$  is the probability that signal  $\mathcal{S}_k$  is preferred by the detector to signal  $\mathcal{S}_i$ , when  $\mathcal{S}_i$  was transmitted. We consider the behavior of the pairwise error probabilities with arbitrary  $\Sigma$  and  $M$  as the SNR approaches infinity, if the order of diversity is full. For the latter to hold, it was shown in [5] that the matrix

$$\begin{bmatrix} \mathcal{S}_i^* \\ \mathcal{S}_k^* \end{bmatrix} [\mathcal{S}_i \quad \mathcal{S}_k] \quad (6)$$

needs to have full rank, for which  $D \geq 2M$  is necessary. Defining  $\mathbf{C}_{ik} = \mathcal{S}_i^* \mathcal{S}_k$ , the pairwise error probabilities approach [5]

$$P_{ik} \sim \binom{2MN-1}{MN} \frac{\bar{\gamma}^{-MN}}{|\Sigma| |\mathbf{I} - \mathbf{C}_{ik} \mathbf{C}_{ik}^*|^N}. \quad (7)$$

The corresponding union bound, denoted as the AUB, is given by

$$\begin{aligned} P^{\text{AUB}} &= \frac{1}{S} \sum_{i=1}^S \sum_{k \neq i} P_{ik} \\ &= \binom{2MN-1}{MN} \frac{\bar{\gamma}^{-MN}}{S |\Sigma|} \sum_{i=1}^S \sum_{k \neq i} \frac{1}{|\mathbf{I} - \mathbf{C}_{ik} \mathbf{C}_{ik}^*|^N}. \end{aligned}$$

The important point here is that in the large SNR regime, the dependence of the bound on the signal geometry (through the determinant  $|\mathbf{I} - \mathbf{C}_{ik} \mathbf{C}_{ik}^*|^N$ ) is decoupled from the fading correlation structure. That means that we can design signals without worrying about the particular correlation structure if we use design techniques based on this large SNR performance measure.

<sup>3</sup>We shall assume that the fading correlation is full rank. If  $\Sigma$  is singular with rank  $r$ , we may form the eigendecomposition  $\Sigma = \mathbf{U} \Lambda \mathbf{U}^*$  with  $\mathbf{U} \in \mathbb{C}^{NM \times r}$ . We can then replace the signals by  $\{\mathcal{S}_i \mathbf{U}\}$  and treat the fading as full rank with correlation  $\Lambda$ .

The eigenvalues of the matrix  $\mathbf{I} - \mathbf{C}_{ik} \mathbf{C}_{ik}^*$  are the squared sines of the  $M$  principal angles between the subspaces  $\langle \mathcal{S}_i \rangle$  and  $\langle \mathcal{S}_k \rangle$  [18]. The principal angles between subspaces can be used in various ways to define a distance measure between complex subspaces (or, equivalently, between points on the Grassmann manifold), see, e.g., [15], [19]. The quantity  $|\mathbf{I} - \mathbf{C}_{ik} \mathbf{C}_{ik}^*|$  is a distance metric between subspaces which has been previously studied in the context of mutual information and statistical inference (see, e.g., [20], [21]).

### IV. SIGNAL DESIGN

To develop an optimality criterion for the signal design problem, we need a numerical function which characterizes (asymptotically) the performance of the detector as a function of the signal constellation. As argued in the preceding section, the probability of error for the Rayleigh-fading channel is asymptotically determined by the function

$$d(\{\mathcal{S}_i\}) = \sum_{i=1}^S \sum_{k \neq i} \frac{1}{|\mathbf{I} - \mathcal{S}_i^* \mathcal{S}_k \mathcal{S}_k^* \mathcal{S}_i|^N}. \quad (8)$$

Notice that this metric differs from the worst case chordal distance employed in [13] and [14], which is defined by

$$d_c(\{\mathcal{S}_i\}) = \min_{k \neq i} \text{tr} \{\mathbf{I} - \mathcal{S}_i^* \mathcal{S}_k \mathcal{S}_k^* \mathcal{S}_i\}. \quad (9)$$

Clearly, optimizing signal constellations over this latter metric does *not* guarantee that full potential diversity order of the space-time channel is achieved, a point which is discussed further in Section VI.

*Problem Statement:* Given  $M, N, D, S \in \mathbb{N}$  ( $\mathbb{N}$  is the set of natural numbers), find the set  $\{\mathcal{S}_i\}_{i=1}^S$  for which the value of  $d(\{\mathcal{S}_i\})$  in (8) is minimized subject to the following constraints: 1)  $\mathcal{S}_i^* \mathcal{S}_i = \mathbf{I}$  for all  $i$ , 2)  $\mathcal{S}_i \in \mathbb{C}^{D \times M}$ .

Since we constrain our signals to have a unitary structure, their properties are completely determined by the  $M$ -dimensional subspace  $\langle \mathcal{S}_i \rangle$  which they span. This means that we may parameterize our optimization over the Grassmannian manifold  $G(M, D)$ , the space of all  $M$ -dimensional subspaces of  $\mathbb{C}^D$ . A parameterization of  $G(M, D)$  that employs  $2MD - M^2$  real parameters is explicitly detailed in [14] following, for example, [22]. However, this parameterization complicates the derivatives of the objective function with respect to its parameters. Consequently, as in [14] (again following [22]), we choose an over-parameterization of  $G(M, D)$ , requiring  $D^2$  real parameters. The latter parameterization is built by expressing any rectangular matrix  $\mathbf{U} \in \mathbb{C}^{D \times M}$  as the product of a square  $D \times D$  unitary matrix and a fixed rectangular  $D \times M$  matrix  $\mathbf{W}$ . Any of the  $D \times D$  unitary matrices can, in turn, be expressed as the product of a real diagonal matrix  $\Phi$  and “simple” unitary matrices  $\mathbf{V}^{pq}(\phi_{pq}, \theta_{pq})$  (complex Givens rotation matrices, each parameterized by two angular parameters and two indices), i.e.,

$$\mathbf{U} = \Phi \left( \prod_{p=1}^{D-1} \prod_{q=D}^{p+1} \mathbf{V}^{pq}(\phi_{pq}, \theta_{pq}) \right) \mathbf{W} \quad (10)$$

where we define the matrix products to be left-sided and the second product decreases its index by minus one for each multiplication. The  $k, l$  element of  $\mathbf{V}^{pq}(\phi_{pq}, \theta_{pq})$  is defined as

$$[\mathbf{V}^{pq}]_{k,l}(\phi_{pq}, \theta_{pq}) = \begin{cases} 1, & k = l, k \neq p, q \\ \cos(\phi_{pq}), & k = l, k = p, q \\ -\sin(\phi_{pq}) \exp(-j\theta_{pq}), & k = p, l = q \\ \sin(\phi_{pq}) \exp(j\theta_{pq}), & k = q, l = p \\ 0, & \text{else.} \end{cases}$$

The AUB provides a smooth differentiable function of these parameters and standard gradient-based optimization may be performed to design the signals. Unfortunately, as the signal set cardinality grows large (corresponding to increasing spectral efficiencies), this optimization becomes infeasible due to the number of free parameters. For this reason, we consider in the next section a suboptimal recursive procedure for approximately optimizing this function.

## V. SUCCESSIVE UPDATES FOR SIGNAL DESIGN

In order to solve the signal design problem of the previous section, an optimization over  $S(DM - M^2)$  parameters describing the signals must be performed, where  $S = 2^{RD}$  with  $R$  denoting the spectral efficiency in bits per complex dimension. In order to allow for a more tractable procedure for large cardinality signal sets, we consider a suboptimal approach, termed *successive updates*.

Suppose that we have already chosen  $K$  signals and seek an additional signal  $\mathbf{S}_{K+1}$  to add to the set such that we increase  $d(\{\mathbf{S}_k\})$  as little as possible. We find that

$$d(\{\mathbf{S}_k\}_{k=1}^{K+1}) = d(\{\mathbf{S}_k\}_{k=1}^K) + 2 \sum_{k=1}^K \frac{1}{|\mathbf{I} - \mathbf{S}_{K+1}^* \mathbf{S}_k \mathbf{S}_k^* \mathbf{S}_{K+1}|^N}. \quad (11)$$

The strategy is to minimize the second term in (11) under the constraint that the additional signal have unit energy  $\text{tr}\{\mathbf{S}_{K+1}^* \mathbf{S}_{K+1}\} = M$ . We initialized each optimization step with a random ‘‘unitary’’ signal. The optimization problem can be parameterized either on the Grassmanian manifold as in Section VI-B or over the usual Euclidean space with an energy constraint on the signals  $\text{tr}\{\mathbf{S}_i^* \mathbf{S}_i\} = M$  (in the examples, we have considered this constraint was sufficient to ensure the stronger structure  $\mathbf{S}_i^* \mathbf{S}_i = \mathbf{I}$ ). We have not seen any major differences between these two techniques, although the Grassmanian parameterization appears nicer numerically since it leads to an unconstrained optimization with a smooth objective function.

It is easy to extend this algorithm to add multiple signals at each iteration. In the limit we have the full optimization problem described in the previous section. We can also use the signals designed with this algorithm to initialize the full, nonrecursive, optimization.

### A. Numerical Results for $M = 1$

We first consider the case of only a single transmit antenna, using the successive updates algorithm with one signal per up-

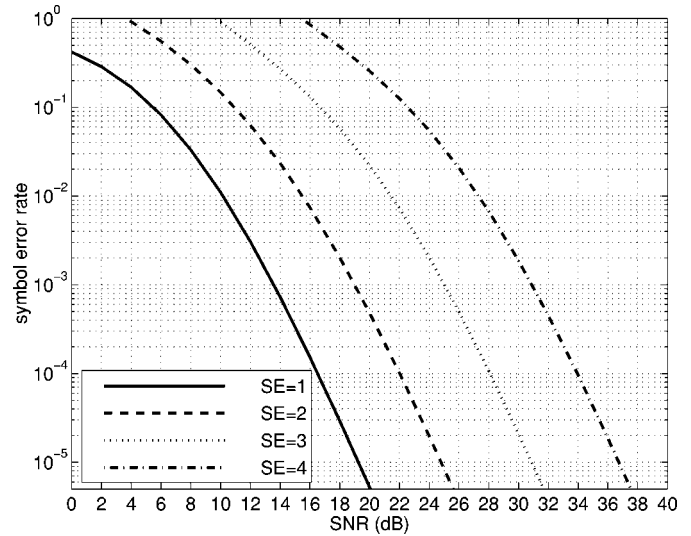


Fig. 1. Probability of symbol error versus SNR for the  $M = 1$  transmit,  $N = 4$  receive antenna channel with  $D = 2$  dimensional signal constellations for several values of spectral efficiency.

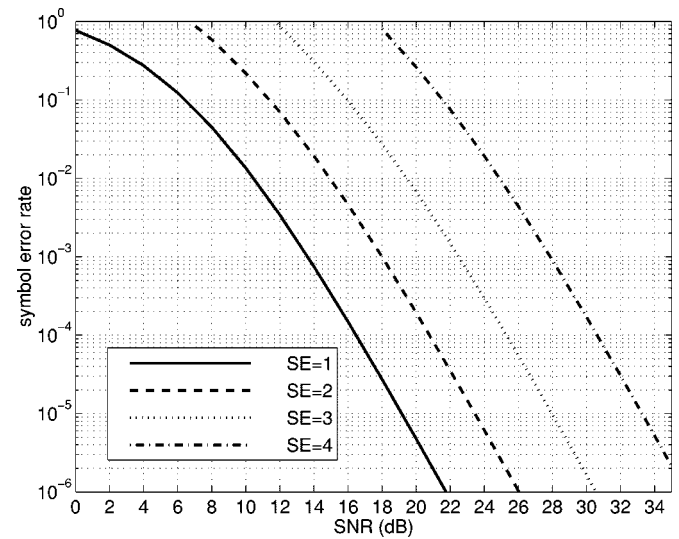


Fig. 2. Probability of symbol error versus SNR for the  $M = 1$  transmit,  $N = 4$  receive antenna channel with  $D = 3$  dimensional signal constellations for several values of spectral efficiency.

date. In Figs. 1 and 2, we plot the probability of symbol error versus the SNR for four receive antennas and  $D = 2$  and  $D = 3$  dimensional constellations for several values of the spectral efficiency. We notice that for the  $D = 2$  design, we incur a 6-dB loss in SNR for every increase by one in the spectral efficiency. This is exactly the behavior predicted in [4] for the capacity of this channel, i.e., that the spectral efficiency should increase by  $M^*(1 - M^*/D)$  bits per second per hertz (b/s/Hz) for every 3-dB gain in SNR, where  $M^* = \min\{M, N, \lfloor D/2 \rfloor\}$ . For the  $D = 3$  dimensional constellations of Fig. 2, this gap is approximately 4.5 dB, again the value predicted for the capacity of this channel. These results imply that our signal designs display a constant SNR gap to capacity for increasing spectral efficiency (at a fixed SER), as expected of optimal constellations.

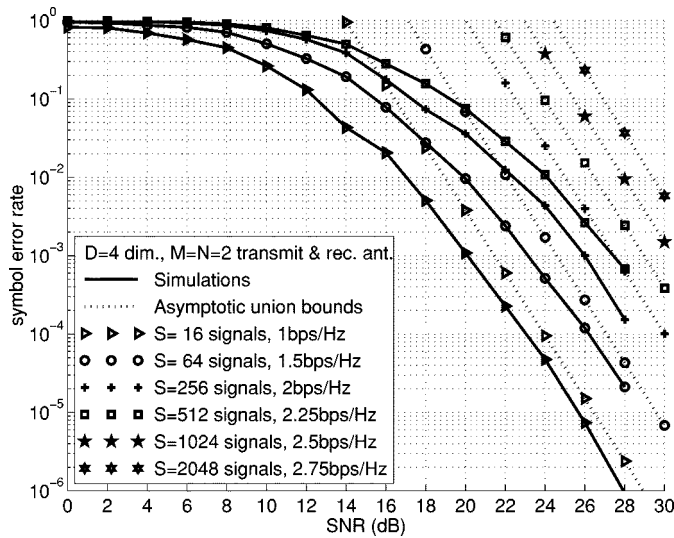


Fig. 3. SER comparison for increasing spectral efficiency for  $M = N = 2$  transmit and receive antennas.

### B. Results for $M = N = 2$

We now present results for multiple transmit and receive antennas. Using the successive updates algorithm with one signal added per update, a signal set with  $S = 2048$  signals in  $D = 4$  dimensions for  $M = N = 2$  transmit and receive antennas was designed. The spectral efficiency of the set is hence 2.75 b/s/Hz. To show the price in energy efficiency for this relatively high spectral efficiency, the performance of the set using only the first 16, 64, 256, 512, 1024 signals, respectively, is also shown in Fig. 3. The figure shows simulated SERs for sets containing up to 512 signals and the AUBs on the symbol error probability for all constellations. Note that the latter are a good indicator of the signals sets' performances. From the figure the price for increasing the spectral efficiency by 1 b/s/Hz (for example, from 1 to 2 b/s/Hz) is roughly 6 dB, indicating a 3-dB penalty when compared to the capacity results in [4].

### C. Results for $M = 2, N = 1$ , With Multiple Signals per Iteration

We end this section with an example demonstrating the utility of adding several signals per iteration. We consider  $M = 2$  transmit antennas,  $N = 2$  receive antennas, and a  $D = 4$  dimensional signal space. In Fig. 4, we plot the AUB for  $S = 128$  signals built with one and with 128 signals per iteration (this latter case corresponds to a joint optimization over all of the signals). We used the signal design for one signal per iteration as an initial guess for the joint optimization problem. We gained about 1 dB in performance through the joint optimization relative to the signal-by-signal update for this example.

## VI. MODIFICATIONS TO EXISTING TECHNIQUES

Most existing signal design techniques for the noncoherent channel employ the worst case chordal bound and can simply be restated with the performance measure in (8). The details of the resulting designs are presented in the subsequent sections.

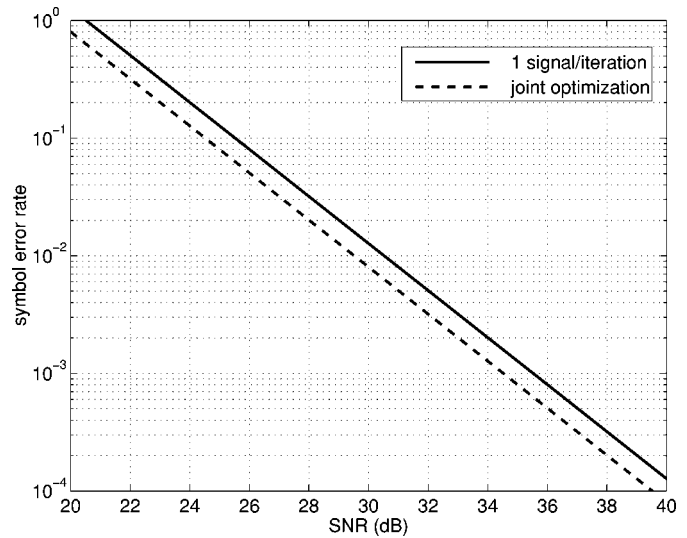


Fig. 4. SER comparison for signals designed with one signal update per iteration and with the joint optimization.

### A. Systematic Designs of Hochwald et al.

In [12], two small signal constellations ( $M = 1$  and  $M = 2$ ,  $S = 32$ ,  $D = 5$ ) were designed based on an iterative “separating” algorithm yielding spectral efficiencies of 1 b/s/Hz. For higher spectral efficiencies, separating two signal points might move them closer to other points, jeopardizing any gains from separating the points.

In [13], larger constellations are systematically generated by starting with an initial signal and successively rotating it. The method is shown to have an algebraic equivalence to block codes in the ring of integers. Signal constellations are found by randomly searching the generating code matrices. The block-circulant structure in the signals simplifies the modulation and demodulation since phase-shift keying (PSK)-type signals are employed (since circulant matrices are diagonalized by the discrete Fourier transform (DFT) matrix [17]), but this structure has to be exchanged for performance (no spectral efficiency higher than 1.5 is reported). Furthermore, the design criterion of maximizing the minimum chordal distance does not necessarily yield good constellations. The generating matrix given in [13] for  $S = 2304$  signals,  $M = 2$  transmit antennas, and  $D = 8$  dimensions does not yield a signal constellation that achieves full order of diversity, since the matrix  $\mathbf{I} - \mathbf{C}_{ik}\mathbf{C}_{ik}^*$  is rank deficient for  $\mathbf{S}_i$  generated from the (algebraic) input vector  $\mathbf{x}_i = [0, 0]$  and  $\mathbf{S}_k$  generated from  $\mathbf{x}_k = [24, 24]$  (because of the cyclic structure of the code, other input vectors yield similar low-rank matrices). With a rather limited random search over the generating matrices (around 2000 matrices in a space of  $48^{12} \approx 1.5 \cdot 10^{20}$  possible generating matrices were considered), we found a generating matrix<sup>4</sup> whose corresponding constellation achieves full order of diversity. Moreover, constellations with nearly the same AUB seem to be quite dense, meaning that several matrices were found which generated roughly equivalent signals. Simulation results comparing the probability of symbol error of each of the two designs is shown in Fig. 5. It is clear that at

$${}^4 \begin{bmatrix} 3 & 26 & 14 & 10 & 2 & 46 \\ 1 & 30 & 39 & 47 & 38 & 16 \end{bmatrix}.$$

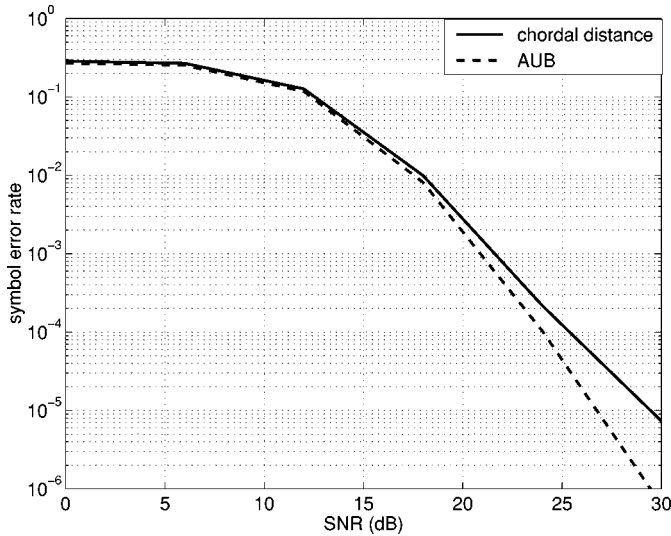


Fig. 5. Simulated SERs versus SNR for the  $M = 2$  transmit,  $N = 2$  receive, antenna channel for the  $S = 2304$  constellation of [13], using the chordal distance on  $G(M, D)$ , and of this section.

high SNRs the effect of reduced diversity is serious, resulting in an ever-widening gap between the performance of the two designs. The minimum chordal distance of our constellation is  $\delta = 0.4062$ , while the one for the generator matrix given in [13] is  $\delta = 0.4427$ , indicating the limited validity of the chordal distance as a figure of merit.

### B. Sphere Packing on the Grassmanian Manifold

In [14], a sphere packing problem on  $G(M, D)$  is described that is essentially the same as the joint optimization described in Section IV with the worst case chordal distance of (9) employed in place of (8). The authors of that paper used a relaxation technique to iteratively approximate the worst case distance by smooth functions of the signal parameters.

A limitation to the sphere packing formulation of the signal design problem is again the use of the minimum chordal distance as the objective function. This not only results in an  $\ell_\infty$  optimization problem but, as mentioned before, it may also not guarantee full diversity order. By using the AUB of (8) we have an objective function which is a smooth differentiable function of the signal parameters and will guarantee that the full diversity order is achieved. We use a gradient search algorithm to solve the design problem, with gradients computed with respect to the Grassmanian parameters as in [14].

## VII. CONVOLUTIONAL CODING

We next consider the use of our signal designs in conjunction with convolutional codes in order to achieve coded modulation schemes with good power-bandwidth efficiencies. We expect these designs to be of the most use for relatively small cardinality constellations, since the resulting Viterbi algorithm requires  $S$  inner products per update and there is no identified structure in our designs to exploit.

Several low-rate convolutional codes for use with orthogonal multipulse modulation (OMM) over single-antenna systems were presented in [16]. The rate  $R = 1/Q$  convolutional

encoder produces a  $Q$ -length sequence of  $S$ -ary output symbols for each  $q$ -ary input symbol with constraint length  $K$  (i.e., each output symbol is a function of the  $K$  most recent input symbols). We may view the codes as a mapping with memory from  $\text{GF}(q)$ , the Galois field of cardinality  $q$ , to  $\text{GF}(S)^Q$ , with  $\text{GF}(q)$  taken to be a subfield of  $\text{GF}(S)$ . This vector of symbols is then read out in serial and mapped to a continuous-time waveform by associating the  $i$ th member of a set of  $S$  waveforms to each output symbol  $i \in \text{GF}(S)$ . The time series of output vectors are related to the input sequence  $u_p$  by the convolutional mapping

$$\mathbf{c}_j = \sum_{k=0}^{K-1} \mathbf{g}_k u_{j-k} \quad (12)$$

where each  $\mathbf{g}_k$  is a  $1 \times Q$  vector with each element lying in  $\text{GF}(S)$  and all arithmetic is done in  $\text{GF}(S)$ .

At the decoder, a sequence of measurements  $\{\mathbf{y}_n(l)\}$  is received with the vector  $\mathbf{y}_n(l)$  corresponding to the  $l$ th code symbol  $\mathbf{c}_n(l)$  of the  $n$ th output vector of the  $P$ -length codeword  $\mathbf{c} = [\mathbf{c}_1 \ \mathbf{c}_2 \ \cdots \ \mathbf{c}_P]$ , so that with  $t = nQ + l$ , we have

$$\mathbf{y}_t = \sqrt{\bar{\gamma}} \mathcal{S}_{c_t} \mathbf{h}_t + \mathbf{n}(t) \quad (13)$$

where  $\mathcal{S}_{c_t}$  is the signal corresponding to the code symbol  $c_t$ ,  $\mathbf{h}_t$  is the fading realization at time  $t$ , and  $c_t = \mathbf{c}_n(l)$  and  $\mathbf{y}_t = \mathbf{y}_n(l)$ . We consider optimal noncoherent decoding with decisions

$$\hat{k} = \arg \max_k \sum_{t=0}^{PQ-1} \mathbf{y}_t^* \mathcal{S}_{c_t^k} \left( \mathbf{I}_{DN} + \bar{\gamma}^{-1} \Sigma^{-1} \right)^{-1} \mathcal{S}_{c_t^k}^* \mathbf{y}_t \quad (14)$$

where  $\{c^k\}$  is the set of allowable codewords. This decoding can be performed in the usual way via a maximum-likelihood trellis search, typically with the Viterbi algorithm. The branch metrics employed in the trellis are given by

$$B_{p,j} = \sum_{t=nQ}^{(n+1)Q-1} \mathbf{y}_t^* \mathcal{S}_{c_t^{p,j}} \left( \mathbf{I}_{DN} + \bar{\gamma}^{-1} \Sigma^{-1} \right)^{-1} \mathcal{S}_{c_t^{p,j}}^* \mathbf{y}_t \quad (15)$$

where  $c^{p,j}$  is the output vector corresponding to the transition from state  $p$  to state  $j$ . The survivor path metric at time  $n$  and state  $j$  is

$$\lambda_n(j) = \max_{p \in \mathcal{G}_j} \{ \lambda_{n-1}(p) + B_{p,j} \} \quad (16)$$

where  $\mathcal{G}_j$  is the set of states that can transition to state  $j$  in one step.

The authors of [16] developed several codes for  $q = 2$  (binary to  $S$ -ary) and  $q = S$  ( $S$ -ary to  $S$ -ary) which are optimal with respect to a truncated information spectrum. That is, they have the largest possible free distance,  $d_{\text{free}}$ , and the best distribution of information symbols,  $N_S(w)$ , associated with remergent trellis paths of Hamming weight  $w$  for  $d_{\text{free}} \leq w \leq d_{\text{free}} + 3$ . They considered performance on the OMM channel with a single transmit and receive antenna. In light of our development of complex correlated  $S$ -ary space-time constellations, we can extend the results of [16] by replacing the orthogonal waveforms in their development by  $S$  signals as designed as in the previous sections.

### A. Two-Codeword Error Probability

We assume that the fading parameters are independent from symbol to symbol (this can be achieved in practice by inter-

leaving and/or frequency hopping, particularly in rapidly fading channels) and that the interantenna fading coefficients within a symbol are i.i.d. so that  $\Sigma = M^{-1}\mathbf{I}$ . This latter assumption is not necessary but will simplify the derivation significantly. The general case is handled along the same lines. Let  $\mathbf{c}^1$  and  $\mathbf{c}^2$  be two codewords generated by the convolutional code which differ in  $w$  positions,  $t_1, t_2, \dots, t_w$ . When the detector of (4) is employed on the  $N$  receive antenna Rayleigh-fading channel we choose  $\mathbf{c}^2$  over  $\mathbf{c}^1$  whenever

$$\sum_{t=1}^w \mathbf{y}_{t_i}^* \mathbf{S}_{c_{t_i}^1}^* \mathbf{S}_{c_{t_i}^2}^* \mathbf{y}_{t_i} - \mathbf{y}_{t_i}^* \mathbf{S}_{c_{t_i}^2}^* \mathbf{S}_{c_{t_i}^1}^* \mathbf{y}_{t_i} < 0. \quad (17)$$

Let us define the vectors

$$\mathbf{z}(k) = \begin{bmatrix} \mathbf{S}_{c_{t_k}^1}^* \mathbf{y}_{t_k} \\ \mathbf{S}_{c_{t_k}^2}^* \mathbf{y}_{t_k} \end{bmatrix}, \quad \mathbf{z} = \begin{bmatrix} \mathbf{z}(1) \\ \vdots \\ \mathbf{z}(w) \end{bmatrix} \quad (18)$$

and let us define the  $2MN \times 2MN$  dimensional matrix  $\mathbf{J}$  via

$$\mathbf{J} = \begin{bmatrix} \mathbf{I} & \mathbf{0} \\ \mathbf{0} & -\mathbf{I} \end{bmatrix}. \quad (19)$$

The maximum-likelihood decoder prefers codeword 2 over codeword 1 whenever

$$\mathbf{z}^* (\mathbf{I}_w \otimes \mathbf{J}) \mathbf{z} < 0 \quad (20)$$

the pairwise error probability is found to be

$$P_2(\{\mathbf{S}_{c_{t_i}^1}\}, \{\mathbf{S}_{c_{t_i}^2}\}) = P[\beta = \mathbf{z}^* (\mathbf{I}_w \otimes \mathbf{J}) \mathbf{z} < 0]. \quad (21)$$

The characteristic function for  $\beta$  can be found using the results of [23, Appendix B], and is given by

$$G_\beta(s) = \frac{1}{|\mathbf{I} + s\mathbf{R}_{zz}(\mathbf{I}_w \otimes \mathbf{J})|} \quad (22)$$

where  $\mathbf{R}_{zz}$  is a block-diagonal matrix with  $k$ th block

$$\begin{aligned} \mathbf{R}_{zz}(k) &= E[\mathbf{z}(k)\mathbf{z}^*(k)] \\ &= \begin{bmatrix} \gamma\Sigma & \mathbf{F}(\mathbf{I} + \gamma\Sigma)\mathbf{C}(k)\mathbf{F} \\ \mathbf{F}\mathbf{C}^*(k)(\mathbf{I} + \gamma\Sigma)\mathbf{F} & \mathbf{F}(\mathbf{I} + \gamma\mathbf{C}^*(k)\Sigma\mathbf{C}(k))\mathbf{F} \end{bmatrix} \end{aligned} \quad (23)$$

and  $\mathbf{C}(k) = \mathbf{S}_{c_{t_k}^1}^* \mathbf{S}_{c_{t_k}^2}$ , and  $\mathbf{F} = (\mathbf{I} + \gamma^{-1}\Sigma^{-1})^{-1/2}$ . Due to the block-diagonal structure of  $\mathbf{R}_{zz}$ , we need only determine the eigenvalues of the  $k$ th block  $\mathbf{R}_{zz}(k)\mathbf{J}$ .

We may use the identity [17]

$$\left| \begin{bmatrix} \mathbf{A} & \mathbf{B} \\ \mathbf{C} & \mathbf{D} \end{bmatrix} \right| = |\mathbf{A}| |\mathbf{D} - \mathbf{C}\mathbf{A}^{-1}\mathbf{B}| \quad (24)$$

to find the eigenvalues of the product  $\mathbf{R}_{zz}(k)\mathbf{J}$ . The eigenvalues are given by the roots of the polynomial

$$\begin{aligned} &|s\mathbf{I} - \mathbf{R}_{zz}(k)\mathbf{J}| \\ &= |s\mathbf{I} - \gamma\Sigma| |s\mathbf{I} + \mathbf{F}(\mathbf{I} + \gamma\mathbf{C}^*(k)\Sigma\mathbf{C}(k))\mathbf{F} \\ &\quad + \mathbf{F}\mathbf{C}^*(k)(\mathbf{I} + \gamma\Sigma)\mathbf{F}(s\mathbf{I} - \gamma\Sigma)^{-1}\mathbf{F} \\ &\quad \times (\mathbf{I} + \gamma\Sigma)\mathbf{C}(k)\mathbf{F}| \end{aligned}$$

$$\begin{aligned} &= |s\mathbf{I} - \gamma\Lambda| \left| \mathbf{U} \left[ s\mathbf{I} + \gamma\Lambda(\mathbf{I} + \gamma\Lambda)^{-1}(\mathbf{I} + \gamma\Lambda\Delta(k)) \right. \right. \\ &\quad \left. \left. + \gamma^2\Lambda^2\Delta(k)(s\mathbf{I} - \gamma\Lambda)^{-1} \right] \mathbf{U}^* \right| \\ &= |s\mathbf{I} - \gamma\Lambda| \left| s\mathbf{I} + \gamma\Lambda(\mathbf{I} + \gamma\Lambda)^{-1}(\mathbf{I} + \gamma\Lambda\Delta(k)) \right. \\ &\quad \left. + \gamma^2\Lambda^2\Delta(k)(s\mathbf{I} - \gamma\Lambda)^{-1} \right| \\ &= \prod_{i=1}^{MN} (s - \gamma\lambda) \left( s + \gamma\lambda \frac{1 + \gamma\lambda |\delta_{1,2}^k(m)|^2}{1 + \gamma\lambda} \right. \\ &\quad \left. + \frac{\gamma^2\lambda^2 |\delta_{1,2}^k(m)|^2}{s - \gamma\lambda} \right) \\ &= \prod_{i=1}^{MN} s^2 - s \frac{\gamma^2\lambda^2(1 - |\delta_{1,2}^k(m)|^2)}{1 + \gamma\lambda} \\ &\quad - \frac{\gamma^2\lambda^2(1 - |\delta_{1,2}^k(m)|^2)}{1 + \gamma\lambda} \end{aligned} \quad (25)$$

where  $\lambda = M^{-1}$  and we have used the unitary decomposition  $\mathbf{C}^*(k)\mathbf{C}(k) = \mathbf{U}\Delta(k)\mathbf{U}^*$ , simplifying the resulting terms to eliminate the matrix  $\mathbf{F}$ . The eigenvalues of  $\mathbf{R}_{zz}(\mathbf{I}_w \otimes \mathbf{J})$  are the roots of these second-order polynomials

$$\{\gamma\eta(k)\} = \left\{ \begin{aligned} &\frac{\gamma^2 (\xi_{1,2}^k(m))^2}{2(M\bar{\gamma} + M^2)} \\ &\pm \frac{\gamma\xi_{1,2}^k(m) \sqrt{\gamma^2 (\xi_{1,2}^k(m))^2 + 4(M\bar{\gamma} + M^2)}}{2(M\bar{\gamma} + M^2)} \end{aligned} \right\}$$

each pair occurring with multiplicity  $N$ . In the above

$$\xi_{1,2}^k(m) = \sqrt{1 - \delta_{1,2}^k(m)}$$

is the square root of the  $m$ th eigenvalue of the matrix  $\mathbf{I} - \mathbf{S}_{c_{t_k}^1}^* \mathbf{S}_{c_{t_k}^2} \mathbf{S}_{c_{t_k}^2}^* \mathbf{S}_{c_{t_k}^1}$ , assumed now to be nonzero since the signal designs yield full diversity order.

The two-codeword probability of error conditioned on  $\{\mathbf{S}_{c_{t_i}^1}\}$  and  $\{\mathbf{S}_{c_{t_i}^2}\}$  is given in terms of the  $2Mw$  eigenvalues  $\{\gamma\eta(k)\}$  by (26), as shown at the bottom of the page. It is the sum over the residues of the negative eigenvalues (see, e.g., [5]). Unfortunately, this pairwise error probability depends on both the Hamming distance  $w$  between the two codewords as well as the particular codewords under consideration. This complicates the specification of the overall bit error probability and precludes the possibility of its computation using the code's transfer function. For this reason, we consider a slightly looser bound in the next section which only depends on the Hamming distance between codewords.

$$P_2(\{\mathbf{S}_{c_{t_i}^1}\}, \{\mathbf{S}_{c_{t_i}^2}\}) = - \sum_{\gamma\eta(k') < 0} \text{Res} \left( \frac{1}{s \prod_{k=1}^w \prod_{l=1}^{2M} \gamma\eta(k)^N \left( s + \frac{1}{\gamma\eta(k)} \right)^N}, s = -\frac{1}{\gamma\eta(k')} \right). \quad (26)$$

### B. An AUB on the Two-Codeword Error Probability

It appears that obtaining an upper bound on pairwise error probabilities that depends only on the weight of the error sequence is a difficult problem. Fortunately, for high SNRs, this problem is tractable. In particular, we consider replacing each pairwise error probability for an error sequence of weight  $w$  by that between the two code sequences of the same Hamming distance that contain the worst case code symbol pair in each of the  $w$  positions in which they differ. This worst case code symbol pair can easily be determined since we know from (8) that for large SNR the corresponding code symbols are the ones that are assigned the two signals that minimize the quantity  $|\mathbf{I} - \mathbf{C}_{ik}\mathbf{C}_{ik}^*|$ . Let  $(\mathbf{S}_i, \mathbf{S}_j)$  be this minimizing pair and let  $\xi^2(m)$  be the  $m$ th eigenvalue of  $\mathbf{I} - \mathbf{C}_{ik}\mathbf{C}_{ik}^*$ . Then we may define

$$P_2^u(w) = - \sum_{\gamma_{k'} < 0} \text{Res} \left( \frac{1}{s \prod_{k=1}^{2M} \gamma_k^{Nw} \left(s + \frac{1}{\gamma_k}\right)^{Nw}}, \frac{1}{\gamma_{k'}} \right) \quad (27)$$

where the  $2M$  eigenvalues  $\{\gamma_k\}$  are given by

$$\{\gamma_k\} = \left\{ \frac{\bar{\gamma}^2 \xi^2(m) \pm \bar{\gamma} \xi(m) \sqrt{\bar{\gamma}^2 \xi^2(m) + 4(M\bar{\gamma} + M^2)}}{2(M\bar{\gamma} + M^2)} \right\}. \quad (28)$$

Consequently, at high SNRs we have

$$P_2 \left( \left\{ \mathbf{S}_{c_i^1} \right\}, \left\{ \mathbf{S}_{c_i^2} \right\} \right) \leq P_2^u(w). \quad (29)$$

### C. An Upper Bound on the Bit Error Probability

Having obtained a pairwise error probability bound which is only a function of the Hamming distance, we can now specify the upper bound on the bit error probability as in the case of orthogonal modulation so that

$$P_b \leq \frac{2^{k-1}}{2^k - 1} \sum_{w=d_{\text{free}}}^{\infty} N_s(w) P_2^u(w) \quad (30)$$

where  $k = 1$  for binary-to- $S$ -ary codes and  $k = \log_2(S)$  for the  $S$ -ary codes. Note that the coefficient that multiplies the infinite sum is taken to be the one that is appropriate for the ‘‘symmetrized’’ channel used to compute the asymptotic upper bound,  $P_2^u(w)$  in (27), for the two-code-sequence error probability.

For the special case of i.i.d. fading with one transmit antenna,  $M = 1$  and  $\mathbf{\Sigma} = \mathbf{I}$ , we have two eigenvalues

$$\{\gamma_k\} = \left\{ \frac{\bar{\gamma}^2 \xi^2 \pm \bar{\gamma} \xi \sqrt{\bar{\gamma}^2 \xi^2 + 4(\bar{\gamma} + 1)}}{2(\bar{\gamma} + 1)} \right\}. \quad (31)$$

Letting  $\gamma_1$  denote the negative eigenvalue we find

$$\begin{aligned} P_2^u(w) &= -\text{Res} \left( \frac{1}{s \gamma_1^{Nw} \gamma_2^{Nw} \left(s + \frac{1}{\gamma_2}\right)^{Nw} \left(s + \frac{1}{\gamma_1}\right)^{Nw}}, \frac{1}{\gamma_1} \right) \\ &= \frac{1}{\left(1 - \frac{\gamma_2}{\gamma_1}\right)^{Nw}} \sum_{k=1}^{Nw-1} \binom{Nw+k-1}{k} \left( \frac{1}{1 - \frac{\gamma_2}{\gamma_1}} \right)^k. \end{aligned} \quad (32)$$

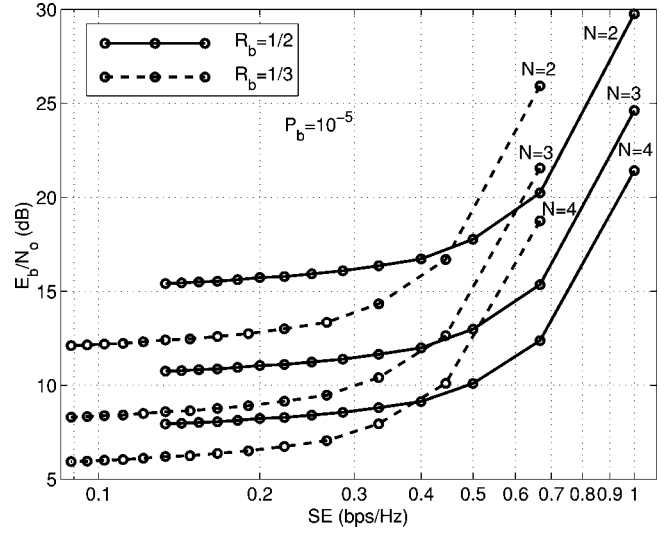


Fig. 6. Energy and spectral efficiencies of the 16-ary convolutional code with constraint length 3 from [16] for varying values of the dimensionality  $D$  on the Rayleigh-fading channel with  $M = 1$  transmit antennas. The curves are produced for  $N \in \{2, 3, 4\}$ , the number of receive antennas.

### D. Asymptotic Behavior of the Code

If we let the SNR grow large, we notice that  $M$  of the  $\{\gamma_k\}$  in (28) approach the constant value  $-1/M$  while the other  $M$  approach the values  $\{\bar{\gamma} \xi^2(m)/M\}$ . This means that we may apply the results of [5] to find the asymptotic form of the two-codeword upper bound

$$P_2^u(w) \rightarrow \binom{2MNw-1}{MNw} \frac{1}{\left(\frac{\bar{\gamma}}{M}\right)^{MNw}} \frac{1}{|\mathbf{I} - \mathbf{C}_{ik}\mathbf{C}_{ik}^*|^{Nw}}. \quad (33)$$

Substituting this bound into (30) we find

$$\begin{aligned} P_b &\leq \frac{2^{k-1}}{2^k - 1} \sum_{w=d_{\text{free}}}^{\infty} N_s(w) P_2^u(w) \\ &\rightarrow \frac{2^{k-1}}{2^k - 1} \sum_{w=d_{\text{free}}}^{\infty} \frac{N_s(w) \binom{2MNw-1}{MNw}}{\left(\frac{\bar{\gamma}}{M}\right)^{MNw} |\mathbf{I} - \mathbf{C}_{ik}\mathbf{C}_{ik}^*|^{Nw}}. \end{aligned} \quad (34)$$

This expression is an infinite polynomial in the inverse SNR,  $1/\bar{\gamma}$ , with leading coefficient of order  $w = d_{\text{free}}$ . We, therefore, interpret the product  $NM d_{\text{free}}$  as the diversity order of the coded space-time scheme and note that  $d_{\text{free}}$  remains the parameter to optimize when designing the convolutional code even when using correlated signaling and multiple antennas. The convolutional code has increased the order of diversity by a factor of the free distance of the code.

### E. Coded Signal Examples

Figs. 6 and 7 show the spectral and energy efficiencies of the 16-ary convolutional codes of [16] for various values of the dimensionality  $D$ , for the independent fading channel with one transmit and two transmit antennas. The signal constellation were designed as in Section V. The constraint length was  $K = 3$  for each code and the generator matrices are given by

$$\mathbf{G}_{1/2} = \begin{bmatrix} 1 & 1 & \alpha^4 \\ 1 & \alpha & \alpha^4 \end{bmatrix} \quad \mathbf{G}_{1/3} = \begin{bmatrix} 1 & 1 & \alpha^4 \\ 1 & \alpha & \alpha^4 \\ 1 & \alpha^2 & \alpha^9 \end{bmatrix} \quad (36)$$

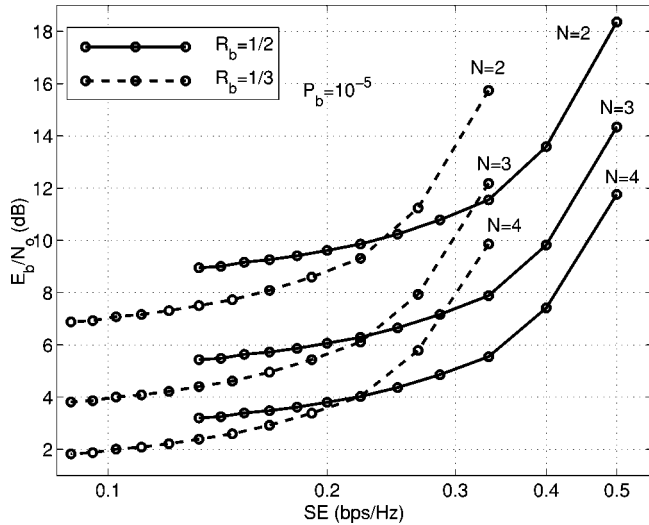


Fig. 7. Energy and spectral efficiencies of the 16-ary convolutional code with constraint length 3 from [16] for varying values of the dimensionality  $D$  on the Rayleigh-fading channel with  $M = 2$  transmit antennas. The curves are produced for  $N \in \{2, 3, 4\}$ , the number of receive antennas.

where  $\alpha$  is a root of  $x^4 + x + 1$  in GF(16). The leftmost point on each curve corresponds to  $D = S$ , for which orthogonal signals are employed, and the rightmost point corresponds to  $D = 2M$ , which is the smallest value of  $D$  for which the full order of diversity may be achieved. The energy efficiencies were calculated by setting the upper bounds on bit error rate in (34) and (32) equal to  $10^{-5}$  (and truncated to the first four terms) and are hence conservative. The key attribute of these plots is that the energy efficiency of the coded signal designs are relatively flat over a large range of spectral efficiencies on the left-hand side of the curves. This result suggests that significant improvements in spectral efficiency can be gained at the expense of relatively small expenditures in transmit power. For example, to increase the spectral efficiency from 1/8 to 1/4 b/s/Hz requires an increase of only 0.25 dB in  $\frac{E_b}{N_0}$  for the rate 1/2 code with  $M = 1$  transmit and  $N = 3$  receive antennas. Similarly, for the same code with  $M = 2$  transmit and  $N = 3$  receive antennas we require an increase of 0.6 dB to move from 1/8 to 1/4 b/s/Hz.

## VIII. CONCLUSION

In this paper, we have presented an approach to noncoherent signal design under dimensionality constraints for the multi-antenna Rayleigh-fading channel based on the AUB. We have introduced a new technique, termed successive updates, that performs the signal design in a recursive fashion. By employing the AUB, we can adapt the techniques of [12]–[14] to better reflect the error probability on the space time channel at large SNRs. The performance of our designs for two and three dimensions was shown to fit well with the theory of optimal designs presented in [4] for the case of single transmit antenna, while a 3-dB gap was seen for the multiple transmit antenna case. This disparity is disappointing but also appears in the designs of [13] and [14].

These signal designs were then coupled with the convolutional codes of [16] to map out new regions of the spectral-energy efficiency plane. The energy efficiency of the resulting codes were seen to be relatively constant over a large range of spectral efficiencies, suggesting that there is a very small loss in using correlated signals as basis waveforms for the codes.

## REFERENCES

- [1] İ. E. Telatar, "Capacity of multi-antenna Gaussian channels," *European Trans. Telecommun.*, vol. 10, no. 6, pp. 585–595, Nov. 1999. Originally, a Nell Laboratories, Lucent Technologies Tech. Rep., Oct. 1995.
- [2] G. J. Foschini and M. J. Gans, "On limits of wireless communications in a fading environment when using multiple antennas," *Wireless Personal Commun.*, vol. 6, no. 3, pp. 311–335, Mar. 1998.
- [3] T. L. Marzetta and B. M. Hochwald, "Capacity of a mobile multiple-antenna communication link in Rayleigh flat fading," *IEEE Trans. Inform. Theory*, vol. 45, pp. 139–157, Jan. 1999.
- [4] L. Zheng and D. N. C. Tse, "Communication on the Grassmann manifold: A geometric approach to the noncoherent multiple-antenna channel," *IEEE Trans. Inform. Theory*, vol. 48, pp. 359–383, Feb. 2002.
- [5] M. Brehler and M. K. Varanasi, "Asymptotic error probability analysis of quadratic receivers in Rayleigh fading channels with applications to a unified analysis of coherent and noncoherent space-time receivers," *IEEE Trans. Inform. Theory*, vol. 47, pp. 2383–2399, Sept. 2001.
- [6] B. Hochwald and W. Sweldens, "Differential unitary space-time modulation," *IEEE Trans. Commun.*, vol. 48, pp. 2041–2052, Dec. 2000.
- [7] V. Tarokh and Jafarkhani, "A differential detection scheme for transmit diversity," *IEEE J. Select. Areas Commun.*, vol. 18, pp. 1169–1174, July 2000.
- [8] B. L. Hughes, "Differential space-time modulation," *IEEE Trans. Inform. Theory*, vol. 46, pp. 2567–2578, Nov. 2000.
- [9] H. Jafarkhani and V. Tarokh, "Multiple transmit antenna differential detection from generalized orthogonal designs," *IEEE Trans. Inform. Theory*, vol. 47, pp. 2626–2631, Sept. 2001.
- [10] D. Warrier and U. Madhow, "Spectrally efficient noncoherent communications," *IEEE Trans. Inform. Theory*, vol. 48, pp. 651–668, Mar. 2001.
- [11] M. L. McCloud and M. K. Varanasi, "Modulation and coding for noncoherent communications," *J. VLSI Signal Processing*, vol. 30, pp. 35–54, Jan./Feb./Mar. 2002.
- [12] B. M. Hochwald and T. L. Marzetta, "Unitary space-time modulation for multiple-antenna communications in Rayleigh flat fading," *IEEE Trans. Inform. Theory*, vol. 46, pp. 543–564, Mar. 2000.
- [13] B. Hochwald, T. L. Marzetta, T. J. Richardson, W. Sweldens, and R. Urbanke, "Systematic design of unitary space-time constellations," *IEEE Trans. Inform. Theory*, vol. 46, pp. 1962–1973, Sept. 2000.
- [14] D. Agrawal, T. J. Richardson, and R. Urbanke, "Multiple-antenna signal constellations for fading channels," *IEEE Trans. Inform. Theory*, vol. 47, pp. 2618–2626, Sept. 2001.
- [15] J. H. Conway, R. H. Hardin, and N. J. A. Sloane, "Packing lines, planes, etc: Packings in Grassmannian spaces," *Exper. Math.*, vol. 5, pp. 139–59, 1996.
- [16] W. E. Ryan and S. G. Wilson, "Two classes of convolutional codes over GF( $q$ ) for  $q$ -ary orthogonal signaling," *IEEE Trans. Commun.*, vol. 39, pp. 30–40, Jan. 1991.
- [17] R. A. Horn and C. R. Johnson, *Matrix Analysis*. Cambridge, U.K.: Cambridge Univ. Press, 1993.
- [18] A. Björck and G. Golub, "Numerical methods for computing angles between linear subspaces," *Math. Comput.*, vol. 27, no. 123, pp. 579–594, July 1973.
- [19] G. Golub and C. F. V. Loan, *Matrix Computation*. Baltimore, MD: Johns Hopkins Univ. Press, 1991.
- [20] I. M. Gel'fand and A. M. Yaglom, "Calculation of the amount of information about a random function contained in another function," *Amer. Math. Soc. Transl.*, vol. 12, 1959.
- [21] L. Scharf and C. T. Mullis, "Canonical coordinates and the geometry of inference, rate and capacity," *IEEE Trans. Signal Processing*, vol. 48, pp. 824–831, Mar. 2000.
- [22] F. D. Murnaghan, *The Unitary and Rotation Groups*, ser. Lectures on Applied Mathematics. Washington, DC: Spartan, 1962, vol. III.
- [23] M. Schwartz, W. R. Bennett, and S. Stein, *Communication Systems and Techniques (An IEEE Press Classic Reissue)*. New York: IEEE Press, 1996. Originally, a McGraw-Hill Publication, 1966.